Copper Transfer from the Cu(I) Chaperone, CopZ, to the Repressor, Zn(II)CopY: Metal Coordination Environments and Protein Interactions†

Paul A. Cobine,‡ Graham N. George,§ Christopher E. Jones,‡ Wasantha A. Wickramasinghe,‡ Marc Solioz,|| and Charles T. Dameron*,⊥

National Research Center for Environmental Toxicology, University of Queensland, Coopers Plains, QLD 4108, Australia, Stanford Synchrotron Radiation Laboratory, Stanford University, SLAC, P.O. Box 4393, Stanford, California 94309, Department of Clinical Pharmacology, University of Berne, 3010 Berne, Switzerland, and Department of Chemistry and Biochemistry, Duquesne University, Pittsburgh, Pennsylvania 15282

Received January 6, 2002; Revised Manuscript Received March 5, 2002

ABSTRACT: Extracellular copper regulates the DNA binding activity of the CopY repressor of *Enterococcus hirae* and thereby controls expression of the copper homeostatic genes encoded by the *cop* operon. CopY has a CxCxxxxCxC metal binding motif. CopZ, a copper chaperone belonging to a family of metallochaperones characterized by a MxCxxC metal binding motif, transfers copper to CopY. The copper binding stoichiometries of CopZ and CopY were determined by in vitro metal reconstitutions. The stoichiometries were found to be one copper(I) per CopZ and two copper(I) per CopY monomer. X-ray absorption studies suggested a mixture of two- and three-coordinate copper in Cu(I)CopZ, but a purely three-coordinate copper coordination with a Cu−Cu interaction for $Cu(I)_2$CopY. The latter coordination is consistent with the formation of a compact binuclear Cu(I)−thiolate core in the CxCxxxxCxC binding motif of CopY. Displacement of zinc, by copper, from CopY was monitored with 2,4-pyridylazoresorcinol. Two copper(I) ions were required to release the single zinc(II) ion bound per CopY monomer. The specificity of copper transfer between CopZ and CopY was dependent on electrostatic interactions. Relative copper binding affinities of the proteins were investigated using the chelator, diethyldithiocarbamic acid (DDC). These data suggest that CopY has a higher affinity for copper than CopZ. However, this affinity difference is not the sole factor in the copper exchange; a charge-based interaction between the two proteins is required for the transfer reaction to proceed. Gain-of-function mutation of a CopZ homologue demonstrated the necessity of four lysine residues on the chaperone for the interaction with CopY. Taken together, these results suggest a mechanism for copper exchange between CopZ and CopY.

The intracellular concentration of copper is tightly controlled, limiting toxic redox-active copper but providing sufficient cofactor for copper-dependent enzymes. Cells balance their safety and requirement for copper through carefully controlled import, export, and sequestration mechanisms. In eukaryotes, the Ctr family of copper transporters takes up copper, while in some bacteria, copper uptake is accomplished by a subclass of P type ATPases, called P1 type or CPx type ATPases (*1*−*3*). Expression and/or localization of the ATPases is regulated by the cellular concentration of copper (*4*). Within the cell, copper is specifically routed to its points of use with the aid of copper chaperones (*5*, *6*).

The *cop* operon of *Enterococcus hirae* is responsible for the regulation of copper uptake, availability, and export in this bacterium. The operon consists of four genes that encode a metalloregulated repressor (CopY), a copper chaperone (CopZ), and two CPx type copper ATPases (CopA and CopB). CopY is a homodimeric repressor that binds to an inverted repeat upstream of the translation start site (*7*). CopZ transfers copper to CopY, thereby releasing it from the promoter and promoting the expression of all four *cop* genes (*8*, *9*).

Current evidence suggests that CopA acts as an import pump under copper limiting conditions, while CopB exports excess copper (*10*, *11*). The import and export ATPase pumps are homologous to the yeast and human/mammalian copper ATPases (*3*). However, CopA and CopB differ in their N-terminal metal binding regions. CopA possesses a metal binding domain homologous to CopZ and the related metallochaperones of yeast (Atx1) and humans (HAH1 or Atox1), while CopB has histidine rich metal binding motifs (*12*, *13*). Such chaperone-like domains are also present in one to six copies in eukaryotic copper ATPases, bacterial cadmium ATPases, and mercuric reductases (*6*). The met-

† Support for these investigations was obtained from the Australian Research Council and Grant 32-56716.99 from the Swiss National Foundation. The Stanford Synchrotron Laboratory is funded by the Department of Energy through the Office of Basic Energy Sciences and the Office of Biological and Environmental Research. The Structural Molecular Biology program is supported by the National Institutes of Health Biomedical Research Technology Program, Division of Research Resources.

* To whom correspondence should be addressed: Department of Chemistry and Biochemistry, Duquesne University, Pittsburgh, PA 15282. Phone: (412) 396-1894. Fax: (412) 396-5683. E-mail: dameron@duq.edu.

‡ University of Queensland.

§ Stanford University.

|| University of Berne.

⊥ Duquesne University.

10.1021/bi025515c CCC: $22.00
Published on Web 04/11/2002

CopY	vetie**C**n**C**ipgq.**C**e**C**kkq
AMT1	msgnmdm**C**l**C**vrgep**C**r**C**harr
Ace1	skedetr**C**r**C**degep**C**k**C**htkr
Mac1	flstq**C**s**C**.edes**C**p**C**vncl
MT-2 β domain	mdpn**C**s**C**atggs**C**t**C**tgsck
Consensus	**CxC(4-5)CxC**

FIGURE 1: Sequence alignment of proteins that have a CxCxxxx-CxC metal binding motif. These proteins are the copper-regulated repressor from *E. hirae* (CopY), the copper-regulated transcription factors from *Candida glabrata* (AMT1) and *Saccharomyces cerevisiae* (Ace1 and Mac1), and the β-domain of the metallothionein from *Homo sapiens* (MT-2 β-domain).

allochaperone-like domains in these proteins have been implicated in the binding of heavy metals for regulation or further processing (*14*). The yeast Atx1 and the human HAH1 chaperones have been demonstrated to route copper to copper ATPases (*15*, *16*). In contrast, CopZ donates copper(I) to the CopY repressor for induction of the *cop* operon (*9*).

The CopZ−CopY interaction is specific. MNKr2, the second domain at the N-terminus of the human Menkes ATPase, is structurally similar to CopZ, but is unable to transfer copper to CopY (*9*). CopZ has the same $\beta\alpha\beta\beta\alpha\beta$ global fold as determined for the copper chaperones Atx1 and HAH1, the mercury chaperone MerP, and the second and fourth metal binding domains of the Menkes copper ATPase (*12*, *17*−*19*). The conserved MxCxxC metal binding motif common to these proteins is a widespread feature of proteins involved in metal ion homeostasis and is also a feature of the multidomain metallochaperone CCS (copper chaperone for superoxide dismutase) (*20*). In contrast, CopY features a CxCxxxxCxC metal binding motif, which is analogous to those of the yeast copper fist transcription factors Mac1 and Ace1, as well as those of metallothioneins, a ubiquitous class of metal detoxification proteins (Figure 1). Copper transfer from CopZ to CopY proceeds from a MxCxxC metal binding site to a CxCxxxxCxC metal binding site. It thus differs from the copper transfer processes between the Atx1 and HAH1 chaperones to copper ATPases, which is a transfer between analogous MxCxxC metal binding motifs (*16*, *21*).

The copper(I) sites in CopZ and CopY are markedly different with regard to solvent exposure; copper(I) binds to CopZ on an exposed loop, while copper(I) binds to CopY is in a solvent-excluded environment (*9*). Key aspects of the copper transfer reaction remain to be established. Here we present the dissection of the individual metal binding sites and demonstrate the importance of charged residues in specific recognition and transfer of copper from the CopZ chaperone to the CopY repressor.

MATERIALS AND METHODS

Protein Purification. CopZ, CopY, MNKr2,[1] and MNKr2K4 were purified to homogeneity by following the previously published methods (*9*, *22*, *23*).

Site-Directed Mutations. The site-directed mutants were prepared using the Stratagene QuikChange kit. Mismatched primers with the corresponding mutations were used with primer extension by the proofreading polymerase *Pfu*I. *Dpn*I digests were used to remove the parental plasmid before transformation into XL-1 blue *Escherichia coli*. The mutants were confirmed by automated dideoxynucleotide sequencing.

Cu(I) Titration of CopZ, MNKr2, and MNKr2K4. Aliquots (10 μM) of the purified apoprotein (CopZ, MNKr2, or MNKr2K4) were titrated with an increasing number of molar equivalents of Cu(I) as $[Cu(I)Cl]_x$ or Cu(I)acetonitrile under anaerobic conditions. The reconstitutions were performed on samples with a reduction state of >95% in accordance with the procedure described previously for metallothionein (*24*) and ACE1 (*25*). Briefly, the reduced apoprotein was mixed at pH 2 with copper(I) and water, after which a concentrated buffer was added (with mixing) to adjust the pH to 8.0. Potassium phosphate buffers were used in the Cu(I) titrations. A Cu(I) stock solution, stabilized as $[CuCl]_x$, was prepared by dissolving CuCl in 0.1 M HCl and 1 M NaCl under anaerobic conditions in a LABCONCO anaerobic chamber or by dissolving Cu(I)acetonitrile in degassed 100% acetonitrile, followed by dilution into degassed distilled water as a working solution. The titrations were monitored by absorption spectroscopy over the wavelength range of 220−820 nm, although only the 220−350 nm range is shown. The broad range was used to ensure that Cu(II)−nitrogen type complexes, which can absorb near 600 nm, were not being produced during the experiments. All spectra were recorded at 23 °C in anaerobically sealed screw-topped fluorescence cuvettes (Spectrocell) containing a total volume of 1.5 mL. After the spectral analysis, the copper concentration was verified by flame atomic absorption spectroscopy in a Varian A-875 series spectrometer. Copper loading of CopZ under native conditions, which results in indistinguishable preparations of Cu(I)CopZ, has also been described previously (*22*).

In Vitro Copper Transfer to CopY. The Cu(I) proteins, prepared as described above, were mixed with Zn(II)CopY in increasing concentrations in 1.5 mL sealed cuvettes. Cu(I) transfer was followed by monitoring the increase in Cu(I)−S luminescence at 600 nm, exciting the sample at 295 nm as reported previously (*9*).

Spectroscopic Analyses. Absorption spectra were recorded on a Cary U3 UV−visible spectrophotometer. Luminescence spectra were recorded on a Perkin-Elmer LS 50B luminescence spectrometer with a 350 nm band-pass filter and settings of 5 and 20 nm for the excitation and emission slits, respectively. The samples were maintained at 23 °C in both instruments.

PAR-Monitored Zinc Displacement. The sequential titration of CopY with Cu(I) results in the displacement of zinc. 2,4-Pyridylazoresorcinol (PAR) has an absorbance maximum at 410 nm, and this absorbance maximum is shifted to 500 nm upon binding of Zn(II). PAR was added to the sequential titration of CopY. The displaced Zn(II) binds to PAR, and the concentration is calculated from the molar extinction coefficient of 8200 M^{-1} cm^{-1} (*26*).

[1] Abbreviations: MNKr2, second amino-terminal copper binding domain of ATP7A representing amino acids 164−181; MNKr2K4, MNKr2 with the four mutations Q38K, R39K, D45K, and N46K; XANES, X-ray absorption near-edge spectroscopy; EXAFS, extended X-ray absorption fine structure; UV−vis, ultraviolet−visible; DDC, diethyldithiocarbamic acid.

Preparation of Samples for X-ray Absorption Analysis. The Cu(I)CopZ X-ray absorption spectroscopy (XAS) samples were prepared with an equimolar Cu(I):protein ratio and a final copper concentration of 0.95 mM. The Ag(I)CopZ sample had a metal:protein ratio of 0.95 and a concentration of 1.1 mM. The Ag(I)CopZ sample was prepared from the apoprotein in 0.1% trifluoroacetic acid in preference to 25 mM HCl because of the solubility problems associated with AgCl. The Cu(I) sample was also prepared from the same apo-CopZ with a perchlorate salt of Cu(I)acetonitrile to avoid any contamination by chloride ions. These samples were reconstituted in 50 mM potassium phosphate (pH 8.0), and 30% (v/v) glycerol was added prior to flash-freezing. The use of these conditions did not affect the titration of CopZ with Cu(I). Cu(I)CopY samples were prepared anaerobically with a metal:protein ratio of 2 and a final copper concentration of 0.8 mM in 100 mM Tris-SO_4 (pH 7.9) containing 40% (v/v) glycerol. Ultrafiltration did not promote changes in stoichiometry, and the recovery of protein was greater than 90%. No excess of reducing agent was added to these samples during preparation because of possible interference in XAS data collection and interpretation.

X-ray Absorption Data Collection. Copper and silver K-edge X-ray absorption spectroscopic data were collected at the Stanford Synchrotron Radiation Laboratory (SSRL) with the SPEAR storage ring containing 50−100 mA at 3.0 GeV. The unfocused wiggler beam line 7-3 was used with the wiggler operating at a field of 1.8 T. A Si(220) double-crystal monochromator was used with an upstream vertical aperture of 1 mm, and harmonic rejection was accomplished by detuning one monochromator crystal to approximately 50% off-peak. The incident X-ray intensity was monitored using an argon (for silver)- or nitrogen (for copper)-filled ionization chamber, and X-ray absorption was measured as the X-ray Kα fluorescence excitation spectrum with an array of 13 germanium detectors (*27*). Samples were maintained at a temperature of approximately 10 K during data collection using a liquid helium flow cryostat. Eighteen 20 min scans were carried out, and the absorption of metal foil standards was measured simultaneously by transmittance. The energy scale was calibrated with reference to the lowest-energy inflection point of the foil, which was assumed to be 8980.3 and 25 515 eV for copper and silver, respectively.

Quantitative analysis of the extended X-ray absorption fine structure (EXAFS) oscillations $\chi(k)$ entailed curve fitting with the EXAFSPAK suite of computer programs (http://ssrl.slac.stanford.edu/exafspak.html) on the basis of ab initio theoretical phase and amplitude functions calculated with the program FEFF version 7.02 (*28*, *29*). No smoothing, Fourier filtering, or related manipulation was performed upon the data. The values for the threshold energy (i.e., energy zero for k) were taken to be 9000.0 and 25 525.0 eV for Cu K-edge and Ag K-edge data, respectively.

Competition Experiments. The relative affinities were determined by competition with the copper chelator diethyldithiocarbamic acid (DDC). The relative affinities were calculated as second-order rate constants using a linear least-squares regression of the observed first-order rate constants plotted as a function of increasing DDC concentrations. The chelator diethyldithiocarbamic acid (DDC) was prepared in sterile MilliQ water as a 1 M concentrated stock. The concentrated stock was diluted to working solutions for titration into the cupro proteins. CopZ, MNKr2, and MNKr2K4 were loaded with copper(I) by the reconstitution method described above. Copper was transferred to CopY from CopZ and MNKr2K4 in the sealed cuvettes, and transfer was confirmed by luminescence. A fixed volume of DDC at varying concentrations was added to the sealed cuvette containing the Cu(I) proteins. Cu(I)DDC was quantified using A_{450} and a molar extinction coefficient of 15 000 M^{-1} cm^{-1}. DDC has no absorbance at 450 nm when not complexed with Cu(I). All spectra were collected using Varian kinetics software and linear least squares calculated using SigmaPlot2000.

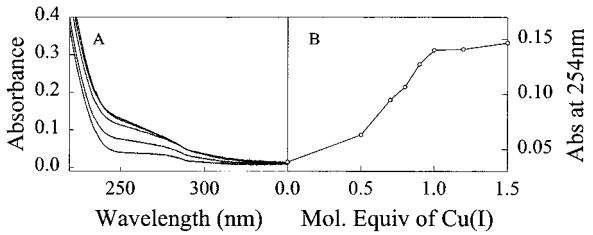

FIGURE 2: Copper(I) loading of the CopZ chaperone. Cu(I)acetonitrile was titrated into apo-CopZ, and the changes in the UV−vis spectra were recorded. (A) Spectra showing the increase at 254 nm due to the formation of a Cu(I)−S metal to ligand charge transfer band. (B) The copper titration curve plotted as the increase in the level of metal to ligand charge transfer vs the equivalents of Cu(I) added to apo-CopZ. The results were the same if $[Cu(I)Cl]_x$ was used as the copper source. Other details of the experiment are described in Materials and Methods.

RESULTS

Cu(I) Titration into CopZ and CopY. To determine the stoichiometry of metal binding to CopZ and CopY, Cu(I) was quantitatively titrated into the purified proteins. Purified CopZ was denatured, reduced, and refolded in the presence of metal ions, followed by spectroscopic analysis of metal complex formation. It has previously been shown by circular dichroism that the reconstituted CopZ (*30*) and other members of this family (*23*, *31*) regain native secondary structure upon refolding. The Cu(I) titration into apo-CopZ suggested that it has a metal binding stoichiometry of one Cu(I) per molecule of CopZ. The UV−vis spectra exhibited an increasing metal to ligand charge transfer band at 254 nm until a plateau was reached at equimolar copper (Figure 2). There were no spectral changes in the 600−800 nm region that would have suggested Cu(II) nitrogen ligands (data not shown). Cu(I)CopZ does not display Cu(I)−S specific luminescence, suggesting the site is exposed to solvent (*9*). In contrast, the Cu(I) in the CxCxxxxCxC binding site of CopY is shielded from solvent, allowing Cu(I)−S luminescence, akin to that observed for the proteins with a homologous metal binding site, ACE1 and AMT (*25*, *32*). The difference in luminescence enables the transfer of copper, from the nonluminescent site in the chaperone CopZ to the luminescent site in the target CopY, to be monitored. Hence, the stoichiometry of copper binding to the repressor protein CopY can be determined with its native Cu(I) source. With sequential addition of Cu(I)CopZ to CopY, the magnitude of the Cu(I)thiolate emission band at 600 nm (excited at 295 nm) increased proportionally until a maximum was reached at a stoichiometry of two Cu(I) atoms per CopY (Figure 3).

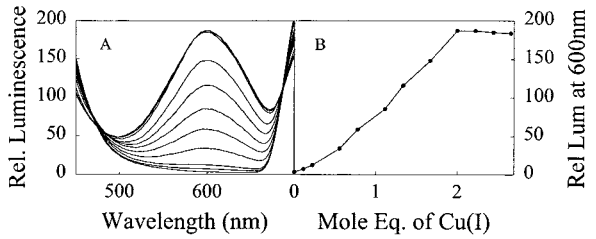

FIGURE 3: Stoichiometry of Cu(I) binding to Zn(II)CopY. Using Cu(I)CopZ as a copper donor, copper was titrated into Zn(II)CopY and the spectral changes due to the formation of Cu(I)CopY were recorded. (A) Emission scans from 450 to 600 nm, using excitation at 295 nm. (B) Plot of emission at 600 nm vs the number of molar equivalents of Cu(I) added as Cu(I)CopZ. Details of the experiment are described in Materials and Methods.

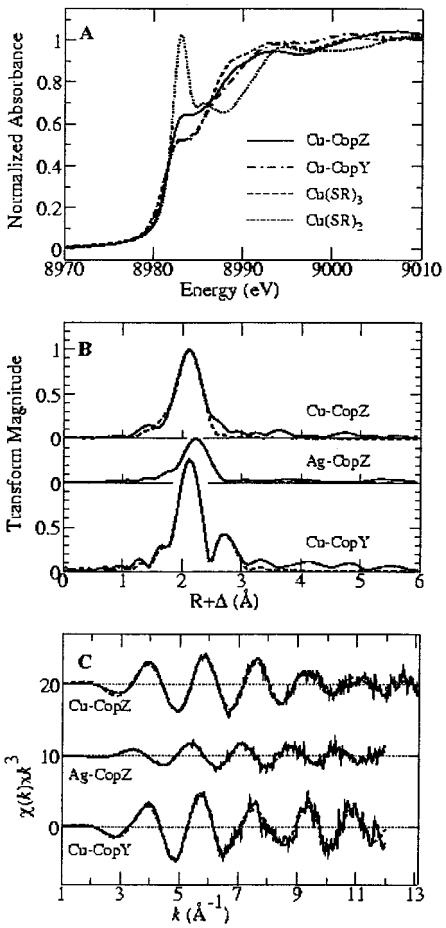

FIGURE 4: XANES and EXAFS for Cu(I)CopZ, Ag(I)CopZ, and Cu(I)CopY. (A) Near-edge spectrum of Cu(I)CopZ and Cu(I)CopY plotted with the spectrum of pure digonal and trigonal species. (B) Fourier transforms for individual Cu(I)CopZ and Cu(I)CopY samples. (C) Respective EXAFS and fits associated with the Fourier transforms. Experimental (—) and fit (- - -).

X-ray Absorption Studies. The metal to ligand charge transfer at 254 nm seen in CopZ was assigned to a copper(I)−sulfur transition. To confirm the cuprous state and the identity of the ligands, X-ray absorption studies were undertaken on Cu(I)CopZ. The Cu K-edge X-ray absorption near-edge spectra displayed no 1s → 3d transition, confirming the presence of Cu(I) (Figure 4A). The near-edge spectrum also exhibited a smaller than expected peak at approximately 8983 eV that would be indicative of purely digonal coordination, which would arise if only the two cysteine sulfurs where involved in binding. The copper EXAFS, best fits, and Fourier transforms are displayed in panels B and C of Figure 4. The spectra are best fit with three Cu(I)−S ligands at 2.241 Å, with no discernible outer-shell EXAFS (e.g., Cu−Cu interactions). Trigonal Cu−S compounds typically have Cu−S bond lengths close to 2.28 Å, while digonal Cu−S compounds have bond lengths of ∼2.15 Å (*33*). The CopZ Cu−S bond length of 2.24 Å is thus only slightly short for a pure trigonally coordinated cuprous site (*33*). The curve fitting analysis yields a rather large σ^2 value of 0.0088 Å^2 for trigonal Cu−S coordination, or 0.0062 Å^2 for digonal coordination. σ^2 is the mean-square deviation of the bond length, and has contributions from both Cu−S vibrations (σ_{vib}^2) and from static disorder in individual Cu−S bond lengths that differ by less than the EXAFS resolution (σ_{stat}^2). Following the methods of George et al. (*34*), we estimate a σ_{vib}^2 of 0.0025 Å^2 and maximum possible σ_{stat}^2 values of 0.0113 and 0.0043 Å^2, for trigonal and digonal copper coordination, respectively (and assuming a chemically homogeneous sample). The total upper bounds for σ^2 are thus 0.0138 and 0.0068 Å^2 for trigonal and digonal coordination, respectively, and our σ^2 estimates, while large, are within a physically reasonable range. O'Halloran and coworkers (*5*) have analyzed the EXAFS of Cu(I)Atx1 and obtained a best fit with two short metal−sulfur bonds 2.25 Å in length and one longer bond 2.40 Å in length. Although the qualitative conclusion of three Cu−S ligands is probably sound, we note that the EXAFS arising from such Cu−S bond lengths is nearly 180° out of phase, and thus close to cancellation and highly correlated, and furthermore at the margin of resolvability. In the case of Atx1, the additional Cu−S bond is potentially added by exogenous thiol added to reduce Cu(II) to Cu(I) in dialysis, or the adjacent methionine in the MxCxxC binding site. Studies using X-ray crystallography, EXAFS, and ^{199}Hg NMR of HgAtx1 and Cu(I)Atx1 and crystallography of reduced Atx1 (*5*, *12*, *35*) have eliminated the latter. Refinements of the Cu EXAFS of CopZ using two short and one long Cu−S bonds resulted in no significant improvement in the fit relative to a single Cu−S shell. The NMR structure of CopZ revealed that the Met group is not within reach of the metal binding cysteine sulfurs (*22*). Furthermore, CopZ samples were prepared in scrupulously sulfur-free buffers.

EXAFS cannot easily discriminate between scatterers of similar size (atomic number); therefore, another possibility is that an external chloride is bound. A large number of Cu(I)(SR)$_2$Cl complexes have been described in the Cambridge Structural Data Base (54 entries). These complexes typically have shorter Cu−S and −Cl bonds than pure thiolate coordination, with average Cu−S and Cu−Cl bond lengths of 2.22 and 2.27 Å, respectively. The presence of chloride is difficult to completely discount, even though great care was taken to exclude it from all buffers and solutions. Curve fitting of the Ag K-edge EXAFS of Ag(I)CopZ gave less ambiguous support for a digonal site. As with Cu(I), Ag(I) has characteristic bond lengths for digonal and trigonal coordination, but with somewhat larger differences; a search of the Cambridge Crystallographic Data Base entries indicates characteristic bond lengths of 2.55 and 2.37 Å for trigonal and digonal coordination, respectively. The EXAFS curve fitting analysis (Figure 4 and Table 1) indicates a best fit with two sulfur ligands, with an Ag−S bond length of 2.39 Å, which is diagnostic of digonal coordination.

Table 1: EXAFS Curve Fitting Results for CopZ and CopY[a]

	M−S			M−M				
sample	*N*	*R* (Å)	σ^2 (Å^2)	*N*	*R* (Å)	σ^2 (Å^2)	ΔE_0 (eV)	error
CuCopZ	3	2.241(2)	0.0096(2)				−16.9(7)	0.314
AgCopZ	2	2.391(5)	0.0079(2)				−17.2(1)	0.394
CuCopY	3	2.256(4)	0.0072(2)	1	2.685(6)	0.0085(6)	−16.9(7)	0.345

[a] *N* is the coordination number. *R* is the mean interatomic distance. σ^2 is the mean square deviation in *R*. ΔE_0 is the threshold energy shift. The fit error is defined as $[\Sigma(\chi_{expt} - \chi_{calc})^2 k^6 / \Sigma \chi_{expt}^2 k^6]^{1/2}$, and the results given are those in which the coordination numbers and Debye−Waller factors were simultaneously refined. The values given in parentheses are estimated standard deviations (precision) obtained from the diagonal elements of the covariance matrix. We note that the accuracy will be larger than these values, and can be assumed to be close to ±0.02 Å and ±0.2 for coordination numbers.

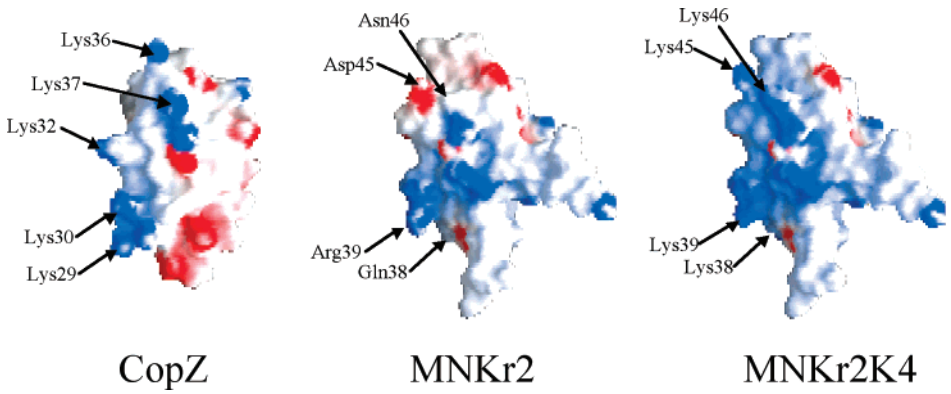

FIGURE 5: Comparison of the positively charged faces of CopZ, MNKr2, and MNKr2K4. The electrostatic surfaces created with GRASP were overlaid onto the NMR structure of CopZ, MNKr2, and a model of MNKr2K4 (*19*, *22*, *43*, *44*). MNKr2K4 was modeled from the average structure of MNKr2 using SYBYL (Tripos). The residues replaced in MNKr2 to create a charged face resembling that of CopZ in MNKr2K4 are labeled.

In contrast to the data for CopZ, the X-ray absorption spectra for two Cu(I) atoms per CopY unambiguously suggest trigonally coordinated Cu(I). The near-edge spectra confirmed the cuprous oxidation state (Figure 4A), and the best fit was obtained with three sulfur backscatterers with a bond length of 2.26 Å, which is very close to the ideal for a trigonal Cu−S bond (*33*). The Fourier transform exhibited an additional peak which curve fitting analysis indicated arises from a copper neighbor at ∼2.69 Å (Figure 4B,C). This coordination is consistent with the CxCxxxxCxC binding site and the formation of a compact $Cu(I)_2$−thiolate core within CopY.

Transfer Specificity. The transfer of copper from Cu(I)-CopZ to Zn(II)CopY is a transient interaction that requires specific recognition. Copper transfer cannot proceed from the identically folded domain of the Menkes ATPase, MNKr2 (*9*). The transfer of copper from the chaperone Atx1 to the similar structured modules of the CCC2 ATPase in yeast has been shown to be dependent on charged residues (*36*). Distinct charged faces exist on the surface of CopZ and MNKr2, but the orientation of the charges is different in the latter (*19*, *22*). Sequence and structural alignment between CopZ and MNKr2 suggests that the differences could prevent an electrostatic interaction between MNKr2 and CopY (Figure 5). Site-directed mutagenesis was used to alter the electrostatic characteristics of MNKr2 so that it would mimic CopZ. A positively charged face was introduced by replacing Q38 and R39, and D45 and N46, in the loop regions between α1 and β2, and between β2 and β3, respectively, with lysine residues. Introducing these four lysine residues conferred the ability to MNKr2K4 to transfer copper to Zn(II)CopY. The transfer of Cu(I) from Cu(I)MNKr2K4 to Zn(II)CopY was monitored using the luminescence assay described above (cf. Figure 3). Figure 6 demonstrates that the metal moves from the nonluminescent site in the mutated Menkes domain to the luminescent environment in CopY. The movement of copper from Cu(I)MNKr2K4 to CopY was independently verified by gel filtration chromatography, as reported previously for the transfer of copper from Cu(I)CopZ to CopY (*9*). Briefly, Cu(I)MNKr2K4 was incubated with Zn(II)-

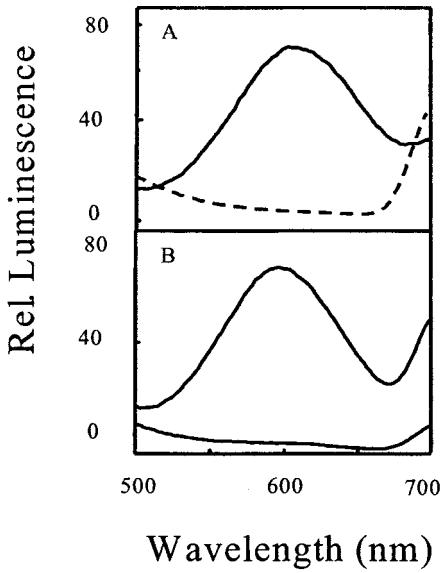

FIGURE 6: Demonstration of copper transfer to CopY as monitored by the formation of a Cu(I) lumaphore in CopY. (A) Emission spectra of Zn(II)CopY preincubated with Cu(I)CopZ (—) and Zn(II)CopY preincubated with Cu(I)MNKr2 (− − −). (B) Emission spectra of Zn(II)CopY preincubated with Cu(I)MNKr2K4 (top) and of Cu(I)MNKr2K4 in the absence of Zn(II)CopY. Details of the experiment are described in Materials and Methods.

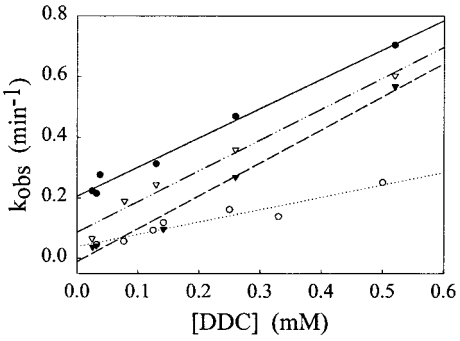

FIGURE 7: Apparent affinity of CopZ, CopY, MNKr2, and MNKr2K4 for Cu(I). The rate of copper extraction from CopZ, CopY, MNKr2, and MNKr2K4 by the chelator DDC was plotted vs the concentration of DDC. The rate of reaction correlates to the affinity of metal binding: CopZ (●), MNKr2 (▼), MNKr2K4 (▽), and CopY (○).

CopY, followed by separation of the two proteins by gel filtration. In the eluate, MNKr2K4 was metal free, the copper was associated with CopY, and the zinc was found in the low-molecular weight fraction. Clearly, copper was quantitatively transferred from Cu(I)MNKr2K4 to Zn(II)CopY (data not shown).

Metal Binding Affinities. The relative copper(I) binding affinities were calculated to support the apparent specificity of the metal transfer reaction. The copper(I) binding affinity indicates the specificity of the copper transfer is related to protein−protein interactions. The similarity of the metal binding sites in MNKr2 and CopZ argues against an affinity difference for these two proteins. However, the transfer characteristics are different. CopY does binds copper in a more cysteine rich site, suggesting an increased copper binding affinity compared to those of CopZ and MNKr2. The mutation of MNKr2 to prepare the lysine rich mutant is not predicted to alter the structure or the metal binding characteristics. Therefore, MNKr2K4 should have an affinity for copper similar to that of native MNKr2. The relative affinities were determined by competition with the copper chelator diethyldithiocarbamic acid (DDC). The rate at which DDC can abstract copper from each protein was used to determine the apparent metal binding affinities of CopY, CopZ, MNKr2, and MNKr2K4. The Cu−DDC complex that is formed absorbs at 450 nm, while the Cu(I)−protein complex has no absorbance at this wavelength. Hence, the rate of removal of Cu(I) by DDC from the Cu(I)-loaded protein can be followed by monitoring the increase in absorbance at 450 nm. The relative affinities were calculated using a linear least-squares regression of the change in observed first-order rate constants plotted as a function of increasing DDC concentrations. Figure 7 shows the rate of DDC copper abstraction from each protein. The slopes correlate with the apparent affinity of the protein for copper in the presence of DDC. CopZ, MNKr2, and MNKr2K4 all have essentially the same slope, $\sim 1.00 \pm 0.07$ mM^{-1} min^{-1}, which suggests that they have similar affinities for Cu(I). In contrast, CopY has a significantly slower rate, 0.40 ± 0.02 mM^{-1} min^{-1}, indicating that the protein resists Cu(I) abstraction by DDC to a greater extent than CopZ, MNKr2, or MNKr2K4. CopY can therefore be considered to have a greater affinity for copper than does CopZ, MNKr2, or MNKr2K4.

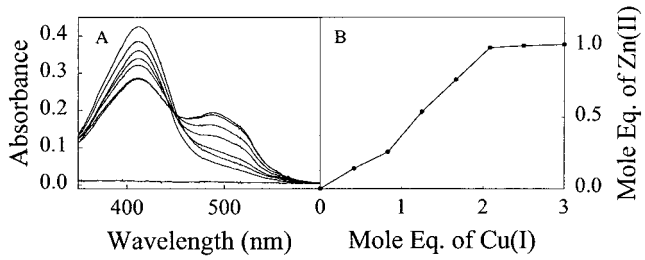

FIGURE 8: Measurement of zinc displacement from CopY by Cu(I)CopZ. The release of zinc from CopY was monitored by the spectral shift of the absorbance maximum from 412 to 500 nm of 2,4-pyridylazoresorcinol (PAR) upon zinc binding. (A) Visible spectra. (B) Number of molar equivalents of Zn(II) displaced vs the number of molar equivalents of added Cu(I)CopZ.

Zinc Displacement from CopY by Copper(I). The transfer of Cu(I) to CopY results in the displacement of zinc from the protein (*9*). The release of zinc was monitored by the spectral shift of the absorbance maximum from 412 to 500 nm of 2,4-pyridylazoresorcinol (PAR) upon zinc binding (*37*). Zinc is presumably bound to the CxCxxxxCxC motif of CopY, which has been shown by EXAFS and the Cu(I)−S luminescence to be the site for copper insertion. PAR by itself was unable to extract Zn(II) from CopY, suggesting that the bound zinc is poorly accessible or that the binding affinity of CopY exceeds that of PAR. PAR titration of copper-induced zinc release by CopY exhibited a stoichiometry of one Zn(II) per CopY monomer, as evident from the plateau in absorbance (Figure 8). Two copper(I) ions displace the zinc quantitatively from this site. Conformational changes associated with this metal exchange are proposed to be the underlying mechanism by which copper promotes the release of CopY from DNA.

DISCUSSION

The *cop* operon of *E. hirae* regulates cytoplasmic copper levels via the encoded CopA copper uptake ATPase and the CopB copper export ATPase. The repressor CopY regulates transcription of the *cop* operon, and the CopZ copper chaperone accepts copper from CopA and delivers it to intracellular targets, including CopY (*9*, *38*). In growth media containing 10 μM copper, the *cop* operon exhibits the lowest observable transcription levels (*7*). Repression is accomplished by binding of Zn(II)CopY to the promoter. If ambient copper rises, the operon is induced by the release of CopY from the promoter. Release of CopY from the DNA is effected by the transfer of two copper(I) ions from Cu(I)-CopZ to CopY, with the concomitant release of the zinc (*9*). This protein-catalyzed delivery of the inducer (copper) to the repressor is novel, and the transfer mechanism is of interest.

Metal titration experiments and luminescence analysis indicated that CopZ binds 1 equiv of Cu(I) in a site that is exposed to solvent. The metal is ligated by the cysteinyl thiolates in a mixed coordination site, as evident from X-ray absorption spectroscopy. The large Debye−Waller factor in these measurements points to considerable static disorder in the Cu(I)−S bond. Cysteinyl thiolates of the conserved MxCxxC motif have been shown to be the ligands for copper in CopZ and in the homologous copper chaperones Atx1 and HAH1 (*12*, *16*, *23*). The distorted linear Cu(I)−S coordination should allow the copper ion to be readily attacked by

other ligands and to be transferred to another protein through a ligand exchange mechanism.

In contrast to the copper(I) environment in CopZ, the two copper(I) ions within CopY are highly sheltered and tightly bound. The luminescence of Cu(I)CopY shows that the Cu(I) ions are ligated to thiolates in an environment that is well-shielded against solvent interactions. Similarly, XAS analysis, XANES and EXAFS, suggested that the copper is three-coordinate with the most likely ligands being thiolates. The Debye−Waller factor for the Cu(I)−thiolate bonds in CopY is indicative of considerably more ordered bonding than in Cu(I)CopZ (Table 1). The Cu−Cu scatter peaks and the limited number of thiolate ligands, four thiolates for two three-coordinate ions, argue for the sharing of ligands. Thiolate bridging or sharing has also been found in other copper(I) cluster proteins, such as the metallothioneins (*39*) or the Cu(I)-regulated transcription factors ACE1 (*25*) and AMT1 (*32*).

A feature of the copper titration of CopY is that the luminescence does not decrease at superstoichiometric copper concentrations. Decreases in luminescence are associated with the incorporation of excess copper(I) and destabilization of the Cu(I) cluster protein structure (*25*, *40*). The inability of CopY to accept excess copper(I) could be due to factors such as loss of recognition of CopZ, stability of the thiolate−Cu(I) cluster, or its inaccessibility. In support of the latter possibility, it was observed that excess copper(I) supplied by Cu(I)acetonitrile is also unable to be incorporated into the site (data not shown).

The individual metal binding properties of the Cu(I) sites in CopZ and CopY reflect the difference in the function of these proteins. Intracellular copper routing demands that the chelation of copper by CopZ be tight enough to prevent deleterious reactions, yet be labile enough for the exchange. The coordination of copper by sulfur in a flexible loop is well-suited for the purpose of copper transfer. The exposed site that provides only two sulfur ligands is suited to ligand exchange reactions facilitating transfer via three-coordinate intermediates when the protein−protein interaction positions the metal binding motifs. The transition from the exposed "leaving" site of CopZ to the more stable, higher-affinity site in CopY could aid in the transfer. Zn(II)CopY would thus behave like a copper sink. This requires the controlled delivery of copper to CopY, presumably involving a specific CopZ−CopY interaction, to prevent uncontrolled copper scavenging by CopY.

CopY, in its active form, is stabilized by a single Zn(II) ion. The displacement of the tetrahedral zinc by two copper(I) ions inactivates CopY repressor activity. The displacement of the zinc by copper, presumed to be the metalloregulatory event, is likely driven by the increased stability of copper(I) ions within CopY. The CopZ−CopY interaction has been postulated to proceed through charged faces on the proteins (*22*). The determined structures of CopZ, HAH1, and Atx1 have all revealed distinct charged faces. Site-directed mutagenesis has highlighted charged residues in Atx1 that are critical to metallochaperone function (*36*). Solution structures of the Cu(I) and apo forms of Atx1 and one of its targets, CCC2a, have allowed the study of the binding interface (*35*, *41*). The CCC2a−Atx1 interaction interface determined by ^{15}N chemical shift mapping confirmed the involvement of charged residues in docking for copper transfer (*42*). The sequence and structure of CopZ show a different pattern of charged residues, and preliminary studies suggest that a charge-based interaction occurs. When MNKr2, normally unable to transfer Cu(I) to CopY, has its surface charge altered through mutations to resemble that of CopZ, it becomes competent to transfer copper. A model is proposed where electrostatic docking occurs away from the metal binding loops and where the flexible loop of CopZ is positioned close enough to allow for ligand attack of one of the metal binding sulfurs of CopY. This leads to a ligand exchange cascade from the less favorable digonal site in CopZ to the more stable trigonal coordination in CopY. The NMR structure of CopZ shows significant changes in the first helix after metal binding (*22*). In this model, the copper transfer from CopZ may promote changes in the positioning of charged residues that allow the dissociation of apo-CopZ and the subsequent interaction of a second Cu(I)CopZ. Clearly, understanding the molecular steps in the Cu(I)CopZ to Zn(II)CopY copper transfer requires further investigation.

ACKNOWLEDGMENT

We thank Professor J. E. Penner-Hahn for generously allowing us access to the XAS spectrum of the digonal cuprous thiolate model compound.

REFERENCES

1. Pena, M. M. O., Lee, J., and Thiele, D. J. (1999) *J. Nutr. 129*, 1251−1260.
2. Lutsenko, S., and Kaplan, J. H. (1995) *Biochemistry 34*, 15608−15613.
3. Solioz, M., and Vulpe, C. (1996) *Trends Biochem. Sci. 21*, 237−241.
4. Camakaris, J., Voskoboinik, I., and Mercer, J. F. (1999) *Biochem. Biophys. Res. Commun. 261*, 225−232.
5. Pufahl, R. A., Singer, C. P., Peariso, K. L., Lin, S.-J., Schmidt, P. J., Fahrni, C. J., Culotta, V. C., Penner-Hahn, J. E., and O'Halloran, T. V. (1997) *Science 278*, 853−856.
6. Harrison, M. D., Jones, C. E., Solioz, M., and Dameron, C. T. (2000) *Trends Biochem. Sci. 25*, 29−32.
7. Strausak, D., and Solioz, M. (1997) *J. Biol. Chem. 272*, 8932−8936.
8. Odermatt, A., and Solioz, M. (1995) *J. Biol. Chem. 270*, 4349−4354.
9. Cobine, P., Wickramasinghe, W. A., Harrison, M. D., Weber, T., Solioz, M., and Dameron, C. T. (1999) *FEBS Lett. 445*, 27−30.
10. Wunderli-Ye, H., and Solioz, M. (2001) *Biochem. Biophys. Res. Commun. 280*, 713−719.
11. Bissig, K. D., Wunderli-Ye, H., Duda, P. W., and Solioz, M. (2001) *Biochem. J. 357*, 217−223.
12. Rosenzweig, A. C., Huffman, D. L., Hou, M. Y., Wernimont, A. K., Pufahl, R. A., and O'Halloran, T. V. (1999) *Structure 7*, 605−617.
13. Klomp, L. W. J., Lin, S. J., Yuan, D. S., Klausner, R. D., Culotta, V. C., and Gitlin, J. D. (1997) *J. Biol. Chem. 272*, 9221−9226.
14. Harrison, M. D., and Dameron, C. T. (1999) *J. Biochem. Mol. Toxicol. 13*, 93−106.
15. Hamza, I., Schaefer, M., Klomp, L. W. J., and Gitlin, J. D. (1999) *Proc. Natl. Acad. Sci. U.S.A. 96*, 13363−13368.
16. Wernimont, A. K., Huffman, D. L., Lamb, A. L., O'Halloran, T. V., and Rosenzweig, A. C. (2000) *Nat. Struct. Biol. 7*, 766−771.
17. Gitschier, J., Moffat, B., Reilly, D., Wood, W. I., and Fairbrother, W. J. (1998) *Nat. Struct. Biol. 5*, 47−54.
18. Steele, R. A., and Opella, S. J. (1997) *Biochemistry 36*, 6885−6895.

19. Jones, C. E., Daly, N., Cobine, P. A., Craik, D., and Dameron, C. T. (2002) *J. Struct. Biol.* (submitted for publication).
20. Lamb, A. L., Wernimont, A. K., Pufahl, R. A., O'Halloran, T. V., and Rosenzweig, A. C. (1999) *Nat. Struct. Biol. 6*, 724−729.
21. Huffman, D. L., and O'Halloran, T. V. (2000) *J. Biol. Chem. 275*, 18611−18614.
22. Wimmer, R., Herrmann, T., Solioz, M., and Wuthrich, K. (1999) *J. Biol. Chem. 99*, 22597−22603.
23. Harrison, M. D., Meier, S., and Dameron, C. T. (1999) *Biochim. Biophys. Acta 1453*, 254−260.
24. Byrd, J., Berger, R. M., McMillin, D. R., Wright, C. F., Hamer, D., and Winge, D. R. (1988) *J. Biol. Chem. 263* (14), 6688−6694.
25. Dameron, C. T., Winge, D. R., George, G. N., Sansone, M., Hu, S., and Hamer, D. (1991) *Proc. Natl. Acad. Sci. U.S.A. 88*, 6127−6131.
26. Griep, M. A., and Lokey, E. R. (1996) *Biochemistry 35*, 8260−8267.
27. Cramer, S. P., Tench, O., Yocum, M., and George, G. N. (1988) *Nucl. Instrum. Methods Phys. Res. 266*, 586−591.
28. Rehr, J. J., Mustre de Leon, J., Zabinsky, S. I., and Albers, R. C. (1991) *J. Am. Chem. Soc. 113*, 5135−5140.
29. Mustre de Leon, J., Rehr, J. J., and Zabinsky, S. I. (1991) *Phys. Rev. B: Condens. Matter Mater. Phys. 44*, 4146−4156.
30. Lu, Z. H., Cobine, P., Dameron, C. T., and Solioz, M. (1999) *J. Trace Elem. Exp. Med. 12*, 347−360.
31. Aronsson, G., Brorsson, A.-C., Sahlman, L., and Jonsson, B.-H. (1997) *FEBS Lett. 411*, 359−364.
32. Thorvaldsen, J. L., Sewell, A. K., Tanner, A. M., Peltier, J. M., Pickering, I. J., George, G. N., and Winge, D. R. (1994) *Biochemistry 33*, 9566−9577.
33. Pickering, I. J., George, G. N., Dameron, C. T., Kurtz, B., Winge, D. R., and Dance, I. G. (1993) *J. Am. Chem. Soc. 115*, 9498−9505.
34. George, G. N., Hilton, J., Prince, R. C., and Rajagopalan, K. V. (1999) *J. Am. Chem. Soc. 121*, 1256−1266.
35. Arnesano, F., Banci, L., Bertini, I., Huffman, D. L., and O'Halloran, T. V. (2001) *Biochemistry 40*, 1528−1539.
36. Portnoy, M. E., Rosenzweig, A. C., Rae, R., Huffman, D. L., O'Halloran, T. V., and Culotta, V. C. (1999) *J. Biol. Chem. 274*, 15041−15045.
37. Giedroc, D. P., Keating, K. M., Williams, K. R., Konigsberg, W. H., and Coleman, J. E. (1986) *Proc. Natl. Acad. Sci. U.S.A. 83*, 8452−8456.
38. Multhaup, G., Strausak, D., Bissig, K. D., and Solioz, M. (2001) *Biochem. Biophys. Res. Commun. 288*, 172−177.
39. Narula, S. S., Winge, D. R., and Armitage, I. M. (1993) *Biochemistry 32*, 6773−6787.
40. Stillman, M. J. (1992) in *Metallothioneins: synthesis, structure and properties of metallothioneins, phytochelatins, and metal−thiolate complexes* (Stillman, M. J., Shaw, C. F., III, and Suzuki, K. T., Eds.) pp 55−127, VCH Publishers, New York.
41. Banci, L., Bertini, I., Ciofi-Baffoni, S., Huffman, D. L., and O'Halloran, T. V. (2001) *J. Biol. Chem. 276*, 8415−8426.
42. Arnesano, F., Banci, L., Bertini, I., Cantini, F., Ciofi-Baffoni, S., Huffman, D. L., and O'Halloran, T. V. (2001) *J. Biol. Chem. 276*, 41365−41376.
43. Nicholls, A., and Honig, B. (1991) *J. Comput. Chem. 12*, 435−445.
44. Nicholls, A., Sharp, K. A., and Honig, B. (1991) *Proteins 11*, 281−296.

BI025515C